Numerical Determination of Gas Velocity and Concentration Fields in Goaf Space of an Underground Hard Coal Mine

Justyna SWOLKIEŃ, ORCID 0000-0003-4332-9415

Nikodem SZLĄZAK, ORCID 0000-0001-8320-4751

Faculty of Civil Engineering and Resource Management, AGH University of Krakow; 30-059 Kraków, Poland; swolkien@agh.edu.pl (J.S.) szlazak@agh.edu.pl (N.S.)

* Correspondence: swolkien@agh.edu.pl

doi: 10.29227/IM-2026-01-01-008

ABSTRACT

The study develops a numerical model of gas flow and composition in a goaf formed after longwall coal extraction. The goaf is treated as a horizontal rectangular porous slab with thickness equal to 3.5 times the mined seam thickness. Air from the mine ventilation system flows into this porous region through adjacent headings, while methane is released from the methane-bearing strata and carbon oxidation occurs within the rubble. The model also includes local nitrogen injection with a specified volumetric flow via a pipeline along the long edge of the goaf. Using the Control Volume Method, the authors compute two dimensional discrete fields in the goaf: overpressure, apparent velocity of the gas mixture, and molar concentrations of nitrogen, methane and oxygen. The resulting computer programs determine these fields for two ventilation layouts, corresponding to typical systems used in longwall mining, each with distinct boundary conditions. This approach enables quantitative assessment of gas migration and distribution patterns in the caving zone, supporting ventilation design and evaluation of methane and oxygen hazards.

KEYWORDS: *velocity field, gas mixture, numerical model, goaf space*

1 INTRODUCTION

A space left after a seam has been extracted, filled with rubble, is called a goaf. Within it, we encounter the movement of the air supplied to the mine and highly variable values of gas concentration. For this reason, research is carried out to describe the processes occurring in goafs.

Two-dimensional airflow models in a goaf space were presented by J. Szlązak and Dieu [1,2] and three-dimensional by Kelsey et al. and Wala et al. [3,4].

The results obtained during numerous experimental studies and modelling have enabled approximate models of a goafs space [5,6,7].

At present, computer programmes created by individual authors are being increasingly replaced by multi-function programming suites for producing simulations using the Computational Fluid Dynamics (CFD).

Applications based on CFD make it possible to determine physical properties of airflow and liquid flow (the distribution of velocity field, the distribution of pressure field), heat transfer (temperature field) and physicochemical processes [8]. For those models, it is vital to determine the properties that characterize the longwalls goaf.

One of the first attempts to model the distribution of permeability in goaf was initiated by Ren and Edwards [9]. They used the permeability values available in the literature, which they next matched to stress values, obtained using the finite element method.

A more comprehensive description of the flow of gas mixtures, taking into account the mutual influence of liquids and solids, was provided by Kelsey et al. [3]. Like their predecessors [9], they associated the anticipated permeability of rock mass affected by mining with the distribution of stresses in the rock mass. However, the stresses were calculated using the FLAC3D (Fast Lagrangian Analysis of Continua) programme, created by Itasca Consulting Group, based on the finite difference method [10]. The obtained picture of permeability was then employed to create a gas migration model in the rock mass, airflow in longwall faces and methane drainage system. Similar research was also conducted by Esterhuizen and Karacan [11], Karacan, Diamond, Esterhuizen and Schatzel [12]. Their model enabled matching permeability to stress values differing by 10 MPa. The changes were applied independently in the horizontal and vertical directions to include the picture's anisotropy or rocks.

The resulting model [13] makes it possible to determine permeability distribution based on its initial values and porosity by applying the Carman-Kozeny equation. The equation was developed theoretically by linking the permeability of a porose medium to its porosity. The Carman-Kozeny equation includes the parameter of the specific surface area, which is usually hard to determine. Moreover, there are fundamental difficulties with determining the value of the Kozeny constant for porose media. Karacan [14,15] concludes that his fractal model is a more accurate tool for determining permeability than the Carman-Kozeny or Happel equations.

The authors studying the airflow in the goaf assume that air and gases' movement occurs within a space whose thickness exceeds three or four times the extracted seam or layer's thickness. The maximum height at which the airflow occurs is referred to as the range of the chaotic caving. According to Znański and Mileticz, the chaotic caving stretches over a threefold thickness of the extracted layer of the seam [16,17]. Besides, the space left after the longwall has been extracted also participates in the airflow. What follows is that the overall height is equal to four times the seam thickness, measured from the seam floor. Considering that the main roof settles by 0.5 to 0.6 of the seam thickness, J. Szlązak assumes that the maximum level at which the airflow takes place in a goaf is equal to 3,5 times the thickness of the extracted layer [1,18]. In that case, the coefficient of permeability assumed within the model has a constant value along the longwall face and at the height of airflow taking place within a goaf.

Here we present a computer-generated simulation of the movement of substance within a porose structure left by the complete extraction of a coal seam through longwall mining in an underground mine. This area is partially ventilated with air supplied by the mine's ventilation system, flowing through excavations at the longwall. Inside the goaf, methane is

released. The calculations also consider the local nitrogen emission with a given volume flow rate, supplied via a pipeline to the caving inside.

The obtained calculation algorithm is based on a *Control Volume Method* procedure, which in Poland has also been referred to as the *Elementary Balance Method.* The most important sources referred to during the formulation of the mathematical model and the algorithm are studies by N. Szlązak and J. Szlązak [19-21].

2 CHARACTERISTIC OF THE GOAF SPACE IN THE HARD COAL MINE

During longwall mining, there occurs a stress concentration in the immediate proximity to the longwall face, resulting from the roof's uncovering and then it's settling in the exploitation area. This process is determined by the roof and the seam's rigidity, the support load-bearing capacity, and the goaf's compressibility.

From the solid to the goaf, five zones can be distinguished with different ranges of extra pressure (σ_z), presented in Figure 1 [22]:

- the intact seam zone, characterized by stress values close to the primary state before exploitation (p_z – the pressure of overlying strata),
- the extraction zone, characterized by higher values of vertical stress,
- the uncovered roof zone, which stretches over the extraction area and often a part of the goaf; in this zone, there is no interaction between the caving and the overlying strata,
- the caving-in-the-sealing-phase zone, including the section of the goaf in which the reaction of the material filling the goaf gradually, increases to reach the value of the primary rock pressure as the distance from the longwall face rises,
- the sealed caving zone, in which the overlying strata are fully supported, which means that the stress values approach the primary state.

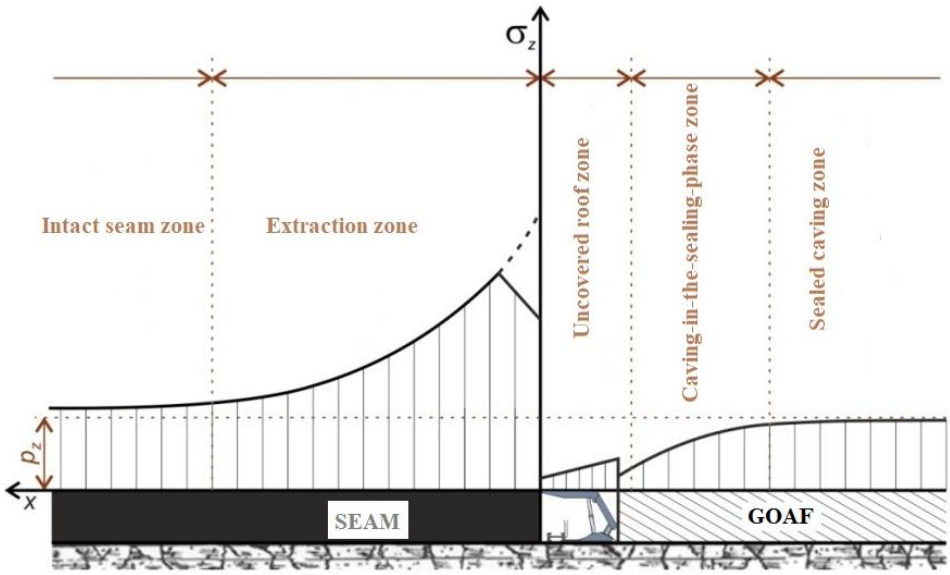

Fig 1. Characteristics of pressure in the rock mass in the longwall area. Adapted from Kłeczek Z. 1994 [22].

From the rock mass mechanics perspective, the goaf is divided into three zones: the caving, the cracks, and the retarded caving (Fig. 2). The present analysis is limited to the caving zone, assuming that it is affected by the pressure drop caused by the leading

ventilation fans. As a result, the zone is an area where the movement of air and gases occurs. The caving zone consists of rocks and possibly the remaining coal that has not been extracted.

The emergence of caving behind an advancing longwall follows the following pattern: the immediate roof above the extracted seam disintegrates into small blocks, which pile up and provide support to the higher roof. Between the blocks, space appears, enabling the flow of air and gases. The resulting rubble forms the so-called caving of the immediate roof. As the longwall advances, the layers above the immediate roof also disintegrate, but into much larger blocks, causing the caving to be fully sealed. As a result of this process, the high caving zone appears. As the longwall continues to advance, the main roof caves in, settling on the blocks in the full caving and high caving zones. At this point, it is essential to add that the rubble near the longwall face does not support the roof. In this area, the overlying rocks' pressure is compensated by the main roof. This process occurs only up to a certain distance from the face, where the rubble supports the roof's rocks.

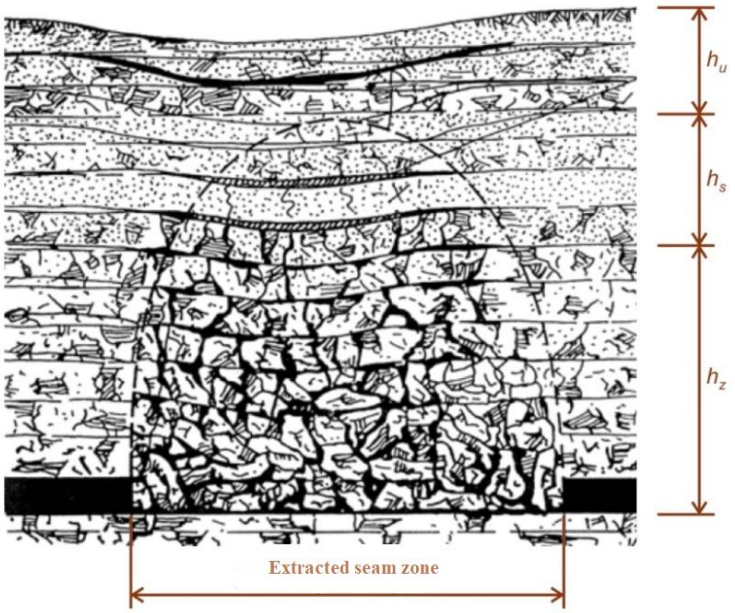

Fig 2. The caving zone (h_z), the cracks zone (h_s), and the retarded caving zone (h_u) that emerged above an extracted longwall

The overall height of a goaf area that emerges from caving, measured by Ropski (full caving and high caving), is from 3.4 to 3.9 times the seam thickness [23]. It is justified to conclude that the flow of the mixture of air and gases in the empty spaces between disintegrated rocks is limited from above by the high caving contact surface and the overlying rocks.

3 THE POROSITY AND PERMEABILITY OF THE GOAF AREA

Goafs' porosity is defined as the ratio of the empty spaces between the rubble, or unsupported roof, to the identified goaf area's overall volume. This area's porosity depends on the following factors [24]: the rocks' structure, their physical properties, and granulometric composition. The blocks of which the rubble of the caving consists can vary in size and

mutual arrangement. The rocks of the main roof, supported by the rubble that constitutes the caving, exert pressure on the blocks, causing them to be sealed. The loosely structured rocks of the caving become increasingly sealed as the distance from the longwall face increases.

The permeability of the goaf is a parameter dependent on its porosity. The relationship between the two properties is determined by the particular rock blocks' geometrical arrangement concerning each other [25]. An analysis of available literature on the subject reveals that changes in porosity and permeability are closely akin.

J. Szlązak [5] presents the results of measurements conducted to identify the influence of how bottom roads are sealed on the airflow through the goaf. The results were analyzed from the relationship between air losses and the type of rocks in the roof. It was found that given the same ventilation conditions, the more compact the rocks in the roof, the greater the air loss values. The study makes it possible to estimate goafs' permeability in a layer with a thickness equal to 3.5 times the extracted longwall thickness.

The experimental research conducted by J. Szlązak [5] considers a classification of cavings based on the so-called 'separation resistance'. The separation resistance is determined by the resistance of rocks to tensile strength, measured in a direction perpendicular to the roof layers' surface. In turn, the resistance of rocks to tensile strength determines their tendency to cave in and disintegrate. Thus, three classes of roofs were distinguished according to their level of separation resistance (Table 1). In describing how the caving zone's height is formed, the separation resistance influences the caving zone height's initial curvature in a plane parallel to the longwall face.

Table 1. Classification of roofs according to separation resistance. Adapted from Szlązak J. 1980; 2000; Szlązak J. and Szlązak N. 2004; 2005 [5,1,26,19]

Roof class	**Separation resistance value (R_s)**	**Roof Description**
	MPa	
Class I	0÷2.5	weak, with cracks, easily caved in (e.g. mudstone)
Class II	2.5÷5.0	self-supporting, without falls, caving in without hanging in goaf (e.g. sandy shale)
Class III	> 5.0	very compact requires breaking up and loosening (e.g. sandstone)

The authors [1,19] determined a coefficient of permeability. Their study reveals that the coefficient of permeability of a goaf decreases as the distance from the longwall face grows. Its highest value was identified near the face, whereas the lowest value of the coefficient was about two-thirds of the face's longwall life. After reaching the minimum, the coefficient starts rising and continues until the beginning of the longwall. As the longwall length increases, the permeability coefficient in this place becomes smaller but is still much higher than the minimum value. As the longwall length increases, so does the goaf section with a small coefficient of permeability.

Goafs with the highest value of separation resistance is characterized by the smallest values of the coefficient of permeability. The greater the separation resistance of the rocks in the roof, the greater the coefficient of permeability.

The statistical analysis of the measured changes of the goafs permeability coefficient has led to the conclusion that it is best described by the following formula [27]:

$$k(x) = \frac{\mu}{r_0 + ax^2} \text{ , m}^2 \tag{1}$$

for $0 \le x \le \frac{2}{3} \cdot l$

where:

μ – coefficient of dynamic air viscosity;

r_0, a – empirical coefficients depending on the geological and mining conditions in the caving;

$k_0 = \frac{\mu}{r_0}$ – coefficient of permeability of the caving behind the longwall face, m^2;

x – distance from the longwall face, m;

l – the length of the extracted section of the longwall, m.

The lowest value of the goaf permeability coefficient is obtained for the value of $x=2/3l$. After reaching its minimum, the permeability coefficient increases up to the place where the longwall begins. For the section characterized by this increase, the approximation can be achieved using the following formula:

$$k(x) = \frac{\mu}{r_0 + a(\frac{4}{3}l - x)^2} \text{ , m}^2 \tag{2}$$

for $\frac{2}{3}l \le x \le l$

The coefficients r_0, k_0, a and b were linked to the rocks' separation resistance in the roof above the extracted seam. Figure 3 presents the coefficients $k_0 = \mu / r_0$ and a dependence on the separation resistance of rocks in the roof.

As the separation resistance grows, so does the value of the coefficient k_0. The change of the caving permeability coefficient behind the longwall face was approximated with the following formula [1]:

$$k_0 = \frac{\mu}{6} 10^{-10} R_{rrs}^{1,44} \text{ , m}^2 \tag{3}$$

where:

R_{rrs} – separation resistance of rocks in the roof, Pa.

The change of the coefficient a was approximated with the following formula [6]:

$$a = 6 \cdot 10^9 R_{rrs}^{-1,74} \text{ , N·s/m}^4 \tag{4}$$

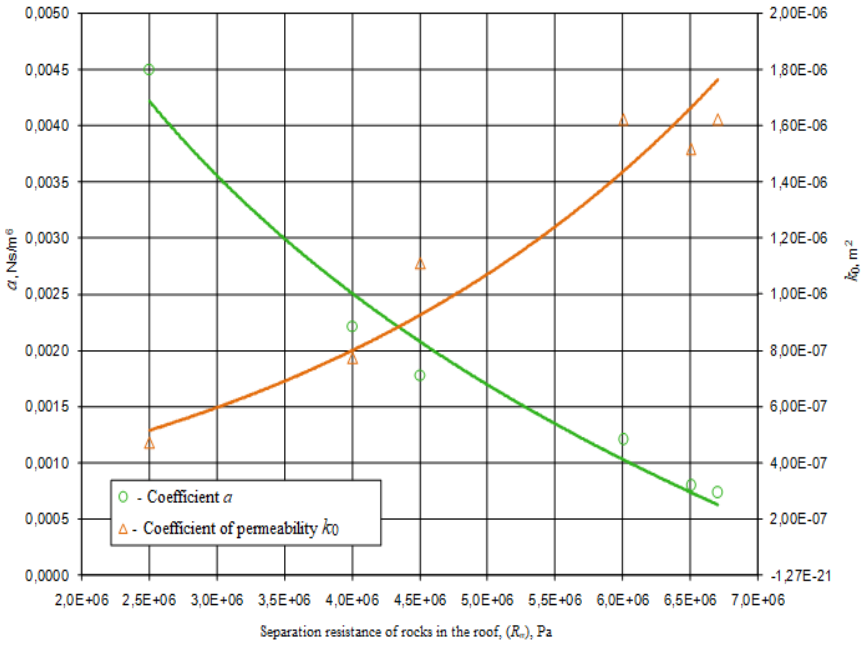

Fig 3. The dependence of the coefficients k_0 and a on the separation resistance of rocks in the roof. Adapted from Szlązak J. 2000, 2001, Szlązak J. and Szlązak N. 2005 [1,27,19]

Figure 4 presents the caving permeability coefficient changes, based on measurements conducted in a mine and approximated using the formulas (1) and (2).

The change of the caving permeability coefficient described by the dependencies above concerns a layer with a thickness equal to 3.5 times the extracted seam's thickness. It implies that the permeability along the vertical axis is constant at the height equal to 3.5 times the extracted seam's thickness. In the conditions of an underground mine, it is impossible to determine the changes of permeability along the vertical coordinate.

A comparison of the Darcy formula with the Blake-Kozeny equation makes it possible to determine the permeability of a layer consisting of spherical solids [20]:

$$k = \frac{d_z^2 \varepsilon^3}{150(1-\varepsilon)^2} \text{ , m}^2 \tag{5}$$

where:

d_z - hydraulic diameter, m;

ε - porosity.

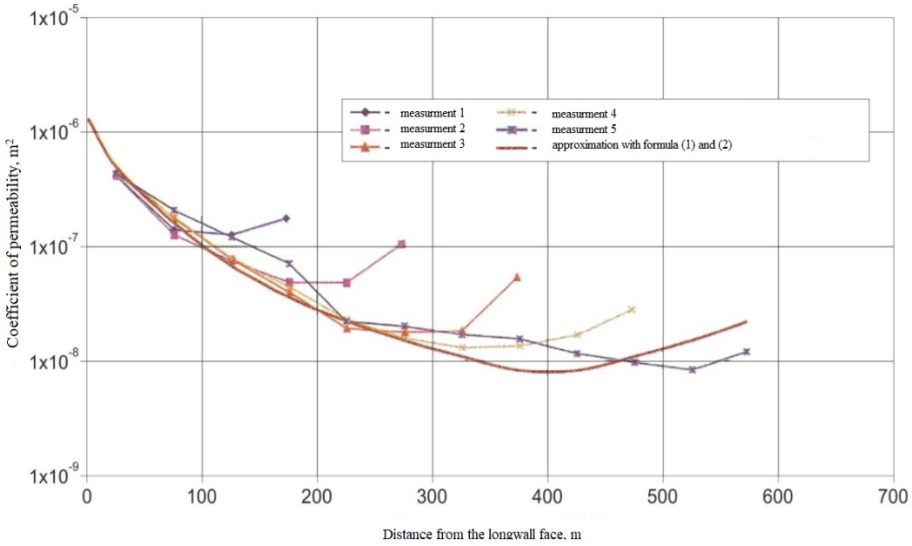

Fig 4. The changes in the caving zone's coefficient of permeability depending on the distance from the longwall face. Adapted from Szlązak J. and Szlazak N. 2005 [19]

Porosity and permeability changes in a cross-section perpendicular to the longwall face resemble the changes in airflow velocity through the goafs of caved longwalls [24,1,19].

At the edges of a goaf, which rest on the longwall supports, a heading, or unextracted rock, porosity and permeability reach their maximum values. Compared to the goaf's middle section, the edge's proximity decreases the roof's rocks' pressure on the caving rocks.

Porosity and permeability are essential for the determination of the distribution of airflow in goafs.

4 THE NUMERICAL DETERMINATION OF THE VELOCITY FIELD AND THE GAS MIXTURE COMPONENTS CONCENTRATION IN A GOAF.

4.1 Research Objectives

The article presents a simulation of the movement of substance within a porose structure left by the complete extraction of a coal seam through longwall mining in an underground mine. The resultant goaf, which remains after a coal seam has been exploited, can be interpreted as a horizontally oriented, rectangular slab with the horizontal dimensions x and y and the vertical dimension 3.5 m, where *m* denotes the thickness of the extracted seam (Figs 5 and 6). In this area, filtration of the air supplied by the ventilation system of the mine takes place, reaching the place through headings adjacent to the horizontal edges of the rectangular block. Inside the goaf, in a porose space, the inevitable complex processes of carbon oxidation occur, and methane is released from the layers permeated with methane. Combined with the oxygen from the atmospheric air, methane can form a dangerous explosive mixture. The rate of methane filtration, and therefore the average capacity of its sources in the caving space, can be approximately calculated based on the prescribed control measurements conducted during the seam's extraction. The calculations also consider the local nitrogen emission with a given volume flow rate, supplied via a pipeline to the inside of the caving along the area's long edge. The simulation yields the following two-dimensional discrete (2-D) physical fields present in the space of the caving:

- field of pressure increase, Pa,

- field of the apparent velocity of the mixture of the components, m/s
- field of the molar concentration of nitrogen N_2, mol/m^3,
- methane concentration field CH_4, mol/m^3,
- oxygen concentration field O_2, mol/m^3.

The created computer programmes enable the determination of the fields mentioned above in two variants with different boundary conditions described below.

The computer programmes were elaborated for the two most frequently used ventilation system:

- the U-shaped ventilation system from the boundaries (Fig. 5);
- the Y-shaped ventilation system (Fig. 6).

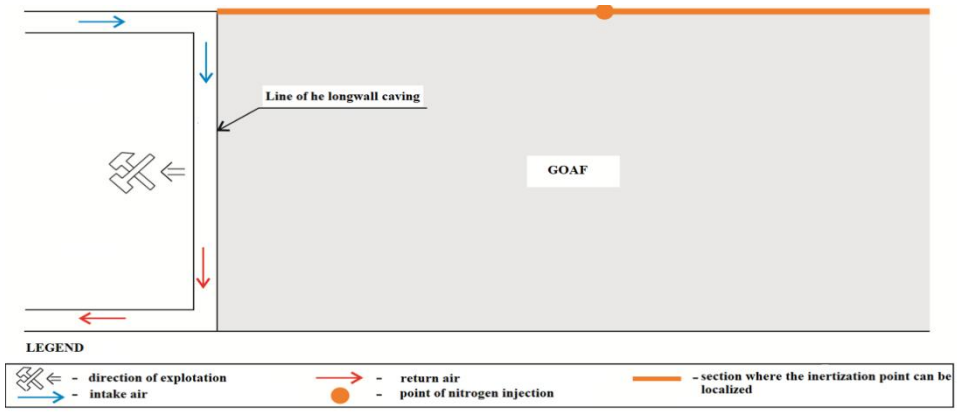

Fig 5. A diagram of the U-shaped ventilation system from the boundaries

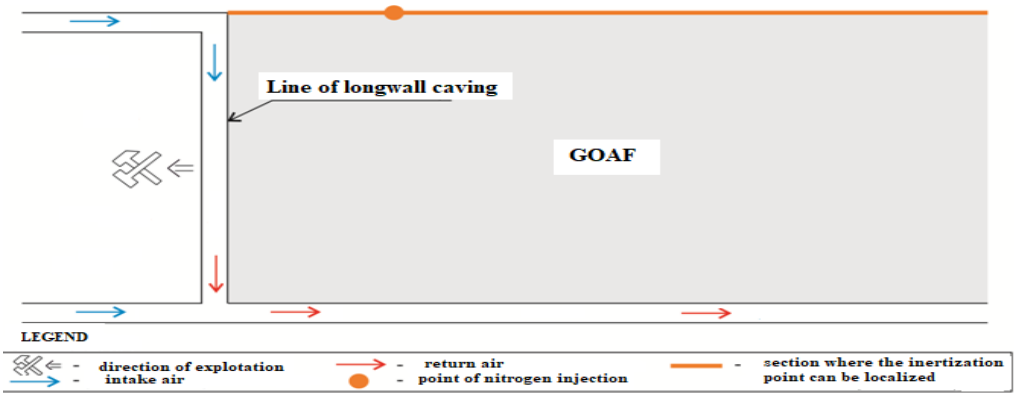

Fig 6. A diagram of the Y-shaped ventilation system

4.2 Theoretical foundations and a general formulation of the mathematical model

An essential factor for the filtration of liquid through a porose medium is the *open porosity*, enabling the pores' space to be penetrated fully by the liquid and constitutes the active area from the flow's perspective. This physical property is closely linked to the permeability of a medium as defined by Darcy's law. In chemical engineering, an assumption of *pseudohomogeneity* is made for such media; however, the assumption is correct only for areas that are significantly (in fact, infinitely) large compared to the size of the pores, or piled pieces of the material. It is justified to believe that in the case of goafs left by the extraction

of coal, this assumption is correct to a sufficient degree. Once pseudohomogeneity is assumed, it becomes possible to define for any point of the porose medium intensive properties concerning both liquids and solids, i.e. density, concentration, coefficients of diffusion, porosity, permeability and others. It is possible, regardless of whether the selected point represents the liquid or the solid phase.

The cross-section area of a porose medium perpendicular to the liquid's penetration's main direction consists of two parts: the cross-section area of the open pores through which the flow passes and the solid cross-section area. The ratio of the former property to the total cross-section area is to a high degree of approximation equal to the medium's above-mentioned open porosity. The so-called *apparent parameters* of the flow are now introduced, including *apparent linear velocity*, the *apparent density of the flow of substance*, and *apparent density of the substance* source. The term 'substance' can denote both a mixture of gas components and each of the components separately. The apparent velocity applies to the medium's total cross-section area, while the real velocity is defined only regarding the active cross-section area. Suppose we assume that the medium's pseudohomogeneity, the apparent velocity can also be determined locally and constitute a vector field. Therefore, it is possible to define apparent densities of flow for both the entire gas mixture and its components. These properties constitute vector fields throughout the entire space of the porose medium. Thus, we obtain the following dependence:

$$\dot{m} = \rho \vec{v} \tag{6}$$

and

$$J_i = -\varepsilon D_i \nabla c_i + \vec{v} c_i \tag{7}$$

where:

m - apparent density of the flow of gas mixture, kg/m^{2}s,

J_i - apparent density of the flow of the i component of the mixture, mol/m^{2}s,

ε - open porosity of the medium m^3/m^3,

D_i - kinematic coefficient of molecular diffusion of the i component of the mixture, whose dependence on the chemical composition of the mixture was neglected for simplification, m^2/s,

ρ - density of the gas mixture, kg/m^3,

c_i - volumetric molar concentration of the i component of the mixture, mol/m^3,

$\vec{v}$ - field of the apparent linear velocity of the mixture within the porose medium, m/s,

$i = 1,2,..N$ - index attributed to a given component of the complex gas mixture,

∇ - *nabla* (a Hamiltonian).

The apparent substance sources densities refer to the porose medium's volume, including both phases and constituting scalar fields within its space.

In the present study, it has been assumed that the filtration of the caving by a gas medium has a laminar nature and that the entire process under consideration is stationary. It is, therefore, possible to describe the local quantity balance for the substance using the following generalized continuity equation:

$$\nabla \cdot \vec{J} = \dot{S} \tag{8}$$

where:

$\vec{J}$ and *S*– generalized densities of the flow of substance (the former) and its internal source in the porose medium (the latter).

Although the principle of mass conservation excludes internal sources of mass, it is acceptable to introduce them as compensating elements in mathematical models' simplifications. In the case under consideration, these sources emerge mainly due to methane reaching the goaf space along the vertical coordinate and possible chemical reactions of the gas and solids' surface inside the pores. By substituting the flow densities defined with the formulas (6,7) for $\vec{J}$ in the equation (8), we obtain the following system of differential equations:

- equation of continuity for the liquid medium,

$$\nabla \cdot \left(\rho \vec{v}\right) = \dot{s}_m \tag{9}$$

- transfer equation for a given component of the liquid,

$$\nabla \cdot \left(\vec{v} c_i\right) = \varepsilon D_i \nabla^2 c_i + \dot{s}_i = 0 \tag{10}$$

for $i = 1,2,..N$,

where:

$\dot{s}_m$ – capacity of the internal source of the gas mixture, kg/m^{3}s,

$\dot{s}_i$ - capacity of the internal source of molar quantity of the *i* component, mol/m^{3}s.

Also, the gas medium filling the pores has to satisfy the state's corresponding equation, which reduces the number of differential equations (10) to the value of $N-1$.

In the case under consideration, because of the medium's compressibility (substantial heterogeneity of its density) and the numerical procedure applied, it is recommended to determine the local composition in the form of mass fractions of the particular components ω_i kg/kg. They enter into the following dependency with the fields of the corresponding values of molar concentration:

$$c_i = \frac{\rho \omega_i}{M_i} \tag{11}$$

where:

M_i – a molar mass of the i component, kg/mol.

The values ω_i satisfy the inequality ‘ $0 \le \omega_i \le 1$ ’ and meet the apparent condition:

$$\sum_{i=1}^{N} \omega_i = 1, \quad i = 1,2,..N \tag{12}$$

After substituting the formula (11) to the equation (10) and the appropriate transformations, we obtain a new system of equations describing the local composition of the gas mixture in the space of a goaf:

$$\nabla \cdot \left(\vec{v}\rho\omega_i\right) = D_i \nabla\left(\varepsilon\rho\nabla\omega_i\right) + D_i \nabla\left(\varepsilon\omega_i \nabla\rho\right) + M_i \dot{s}_i \tag{13}$$

The equation system (9,13) is an indeterminate one because the number of unknown functions is higher than the number of equations in the system. The system can be solved by incorporating the equation of state for a liquid medium, and by introducing Darcy's equation, which in the case of a horizontal goaf area assumes the following form:

$$\vec{v} = -\frac{k}{\mu}\nabla\pi \tag{14}$$

Where:

k – permeability of a porose medium (determined based on dependencies (1 and 2)), m^2, μ - dynamic coefficient of viscosity of the gas mixture, kg/ms,

π – overpressure field (pressure increase concerning the external atmospheric pressure p_0) in the space of the pores, Pa.

The pressure p_0 is determined for the heading cross-section in which the air leaves the area under analysis. That means the following condition $\pi \geq 0$ is always met. Given the above, the total local pressure within the goaf area is $p = p_0 + \pi$ Pa. This value is an established parameter within the model and incorporated in the calculations as part of the input.

By substituting the apparent velocity described with the formula (14) to the equation (9), we obtain the following differential equation, which can be used to determine the pressure field in the space of the goaf, provided that appropriate boundary conditions have been defined:

$$\nabla \cdot \left(K\nabla\pi\right) + \dot{s}_m = 0 \tag{15}$$

where:

$$K = \rho\frac{k}{\mu} \tag{16}$$

In most cases, the medium filling the pores' internal spaces is a mixture of mine air and methane. Therefore, it can be assumed that in the thermal conditions of a mine, it behaves like a semi-ideal gas and satisfies the equation proposed by Clapeyron to a sufficient degree. By applying Dalton's law, it is possible to reach a formula that defines the density of gas mixture as a function of the total pressure and the composition of the gas mixture:

$$\rho = \frac{p_0 + \pi}{RT\sum_{i=1}^{N}\frac{\omega_i}{M_i}} \tag{17}$$

Where:

T – local absolute temperature ($\cong 298{,}0 = const$), K,

R - universal gas constant ($\cong 8{,}315$), J/molK.

Given the necessity to meet the condition (12), the number of equations having the form (13) is reduced from N to $N-1$, because the concentration field of a single, appropriately selected component of the mixture is defined directly by an equation expressing the condition above. As a result, the system of differential equations describing the transfer of substance inside goafs left after extracting a seam consists of the following equations:

- continuity equation having the form of (15), (quantity: 1),
- equations of convection-diffusion transport of the individual gas components having the form of (13), (quantity:' $N-1$ '),
- the equation expressing the condition (12), (quantity: 1).

Solving the above system of equations for the area under consideration leads to obtaining values for the following properties (in the given order): π overpressure field, fields of mass fractions ω_i for $N-1$ gas components, the mass fraction field for the N-th gas component.

All the values on the right-hand side of the formula (16) constitute heterogenous scalar fields in a goaf space. The variable nature of the properties ρ and μ results from the complex chemical composition of the gas medium penetrating the goaf, whereas permeability k is a function of only the horizontal spatial variable parallel to the longer side of the rectangular area under analysis, which is confirmed by research conducted by N. Szlązak and J. Szlązak (2005) [19]. Knowing the value of k, it is possible to estimate the local value of open porosity ε, assuming that the caving is a piled layer consisting of solid grains with a substitute diameter d_z, m. For this purpose, the approximate Blake-Karman formula is applied [20].

The gas mixture density as a function of pressure and mass composition is defined by the formula (17). The mixture's dynamic viscosity as a function of its chemical composition can be determined quite accurately using Wilke's algorithm [20]. As has already been said, the vertical dimension (the thickness of the caving layer) is negligibly small compared to the horizontal dimensions, which justifies the assumption that the problem under analysis is a two-dimensional one.

A separate challenge is how to define the boundary conditions for the equations (13,15). For this purpose, it is necessary to know the chemical composition and the gas medium's pressure flowing through the headings adjacent to the mining area. Of course, this medium consists mostly of air supplied by the ventilation system, locally containing methane released from the goaf. The data needed to determine the boundary conditions can be obtained through appropriate airflow measurements along the heading. However, this option limits the possibility of generalizing the results of the simulation. For this reasons, it is useful to add to the system (12,13,15) differential equations describing the profiles of pressure and concentration along the spatial coordinate ξ, m, situated in the longwall working and pointed in the direction of the airflow. Along its entire length, this coordinate is perpendicular to the cross-section of the heading. It is also situated on the perimeter of the rectangular goaf area, covering part of its edge. The point $\xi = 0$ marks the beginning of the corridor, which is also the inlet of air. As we know, the flow of air along a heading is always turbulent. It can be roughly interpreted as fully developed for the entire length of the discussed coordinate ξ. Because of turbulent fluctuations, the obtained values of mass fractions and pressures corresponding to the stationary condition are (following Reynolds' hypothesis) averaged in

time. The turbulent core occupies the entire area of the heading's cross-section, which means that the sought-after values, including the vector of the airflow velocity averaged in time, are only a function ξ form flat, homogenous fields in the cross-sections. The assumption that the airflow is fully developed appears to be justified despite the exchange of mass at the caving surface, connected with the goaf's filtration by the air and methane release. This is because the mass flows at this surface are negligibly small compared to the mass flow of air moving along the heading. Also, the hydrodynamic layers (turbulent and laminar) at the walls are absent because of the processes mentioned above and the surface's considerable irregularity.

In the mathematical model section concerning the transfer of mass in headings adjacent to goafs, the sought-after properties, i.e. overpressure, linear velocity of the gas medium, and mass fractions of the components are designated with capital letters: Π, $\vec{V}$, and Ω_i (respectively). During the airflow analysis in the heading, it was possible to determine pressure distribution along the coordinate using hydraulic resistance. Due to the one-dimensional character of the airflow, parameters used to describe it, such as total pressure and linear velocity averaged in time and on the cross-section area, satisfy a sufficiently good approximation the Darcy-Weisbach equation. It can then be presented in the following form:

$$\frac{p_1 - p_2}{L} = \gamma \frac{\rho (V_\xi)^2}{2 d_z} \tag{18}$$

Where:

V_ξ, m/s is the velocity of the gas medium along the coordinate ξ,

The properties p_1 and p_2, Pa denote the values of total (atmospheric) pressure at the opposite ends of the heading with the length L and substitute (hydraulic) diameter d_z, m, while γ, m^{-3}, represents the so-called coefficient of hydraulic resistance. The equation above can also have a differential form because the left-hand side represents a difference quotient of pressure concerning the coordinate ξ. Also, if we consider that $p = p_0 + \Pi$ we get:

$$V_\xi = -\mathrm{E} \frac{d\Pi}{d\xi} \tag{19}$$

where E, as a value inversely proportional to hydraulic resistance, can to some extent be interpreted as a measure of the permeability of the gas in the heading. The equation (18) implies that the formula expresses the discussed value:

$$\mathrm{E} = \frac{2 d_z}{\gamma \rho V_\xi} \tag{20}$$

and is the equivalent of the coefficient 'k/μ' in the formula (11). Based on transformations similar to those applied for equations (9,11), we obtain the following ordinary differential equation defining the profile of pressure along the length of the heading:

$$\frac{d}{d\xi}\left(K_b \frac{d\Pi}{d\xi} \right) + \dot{s}_{bm} = 0 \tag{21}$$

where $K_b = \rho E$, $\dot{s}_{bm}$ denotes the mass source capacity within the space of the heading, kg/m^{3}s, while the index 'b' symbolizes points situated at the edge of the goaf area. As explained above, the presence of mass sources in the equation (21) reflects the filtration of the caving by air and methane release. Both hydrodynamic processes co-occur simultaneously at the inner surface of goafs. The property $\dot{s}_{bm}$, which is a function of the coordinate ξ, can be determined using Darcy's law (14):

$$\dot{s}_{bm} = -\frac{K}{d}\frac{\partial \pi}{\partial n} \tag{22}$$

where:

d - heading width, m,

n - spatial coordinate, surface normal to the surface of the goaf area's boundary, pointed 'from the inside to the outside', m, whereas the property K is expressed with the formula (16). It should be noted that both the directional derivative and the values defining the parameter K, i.e. k, ρ and μ, are defined only for those sections of the edge of the caving that have direct contact with the gas medium's flow through the heading.

The boundary conditions for the equation (21) are defined for the extreme heading points i.e. for $\xi = 0$ (the inlet of air that is not polluted with methane) and for $\xi = \xi_k$ (the outlet of the gas medium consisting of nitrogen, oxygen and methane).

The boundary condition for the inlet of fresh air with atmospheric composition assumes the following form:

$$-E\frac{\partial \Pi}{\partial \xi} = V_{\xi 0}, \qquad \text{for } \xi = 0 \tag{23}$$

where:

$V_{\xi 0}$ – linear velocity of airflow at the inlet's cross-section to the heading, m/s, (the property is part of the input data for calculations within the model).

As for the outlet ξ_k, the following dependency applies:

$$\Pi = 0, \qquad \text{for } \xi = \xi_k \tag{24}$$

By solving the equation (21) containing the source member (22) with the boundary conditions (23,24) satisfied, we obtain the distribution of overpressure $\Pi(\xi)$ along the heading, which in turn makes it possible to formulate the boundary conditions for the continuity equation (15). Therefore, for the surface of mass exchange between the goaf and the medium flowing along the heading, the following Dirichlet boundary conditions apply:

$$\pi = \Pi \tag{25}$$

A similar analysis is carried out to determine the distributions of molar fractions of the gas medium's individual components along the heading's length, i.e. the function $\Omega_i(\xi)$ for

$i = 1,2,...N-1$. For this purpose, it is necessary to solve a system of equations having the form (13); in this system of equations, the turbulent diffusion of the components along the direction of the airflow is neglected for simplification, only the convectional form of transport being considered. Given the one-dimensional nature of the problem, the following ordinary differential equation is obtained:

$$\frac{d}{d\xi}\left(V_{\xi}\rho\Omega_i\right) + M_i\dot{s}_{bi} = 0 \tag{26}$$

where the presence of the source member $\dot{s}_{bi}$, mol/m^{3}s – like in the case of equation (21) – is a consequence of the exchange between the gas medium in the heading and the goaf's surface. Depending only on ξ, this property is determined based on formulas (7) and (11), referring only to the caving sections directly contacting the heading. After the appropriate transformations, the following dependence is obtained:

$$\dot{s}_{bi} = \frac{1}{M_i d}\left(-\varepsilon_b D_i \rho \frac{\partial \omega_i}{\partial n} - \varepsilon_b D_i \omega_i \frac{\partial \rho}{\partial n} + v_n \rho \omega_i\right) \tag{27}$$

where:

ε_b - the open porosity of the goaf in the immediate proximity to the heading,

v_n - linear velocity of the medium filtrating the goaf at the edges, m/s, while $i = 1,2,...N-1$.

As for the first-order differential equations having the form of (26), it is sufficient to formulate a boundary condition at the gas medium's inlet into the corridor. Thus, we obtain:

$$\Omega_i = \Omega_i^0 \text{ for, } \xi = 0,\ i = 1,2,...,N-1 \tag{28}$$

where Ω_i^0 denote the mass fractions of gas components at the entry. For the known molar composition of the analyzed medium, provided as input data, values for the components are determined during the preliminary phase of the calculations, based on the known values of their molar mass M_i. The local density ρ is determined using the formula (17), in which the values π, ω are replaced with the values Π and Ω. Overpressure Π at the inlet is determined by solving the equation (21).

Solving the equation (26) containing the source member (27) with the consideration of the boundary condition (28) makes it possible (as was the case with the overpressure field) to formulate Dirichlet boundary conditions for equations (13):

$$\omega_i = \Omega_i \qquad \text{for} \qquad i = 1,2,...,N-1 \tag{29}$$

It is assumed that at those sections of the goaf edges that do not have contact with the flowing air there is no transfer of substance across the boundary surface That leads to the formulation of the following Neumann boundary conditions:

$$\frac{\partial p}{\partial n} = 0 \tag{30}$$

and

$$\frac{\partial \omega_i}{\partial n} = 0 \qquad \text{for} \qquad i = 1,2,...N-1 \tag{31}$$

The field of mass fraction of the N-th component inside the goaf and in the heading space is calculated using the equation (12).

At this point, it is necessary to notice the interdependence of the differential equations (13,15) and (21,26). The formula (17) links each of them so as functions defining substance exchange at the edge of the caving (formulas (21), (27) and (29)). In this connection, given the unavailability of an analytical solution to the non-linear boundary-related problem formulated above, it is necessary to apply a numerical procedure adapting appropriate iterative methods.

4.3 The details of the equations in the mathematical model

Because of the rectangular shape of the area under analysis, a Cartesian coordinate system was employed. The differential equations (13) and (15) were formulated in a two-dimensional (2-D) form in a changed order, corresponding to the accepted method of solving them. Thus, we obtain:

$$\frac{\partial}{\partial x}\left(K\frac{\partial \pi}{\partial x}\right) + \frac{\partial}{\partial y}\left(K\frac{\partial \pi}{\partial y}\right) + \dot{s}_m = 0 \tag{32}$$

$$v_x = -K\frac{\partial \pi}{\partial x} \quad \text{and} \quad v_y = -K\frac{\partial \pi}{\partial y} \tag{33}$$

$$\frac{\partial}{\partial x}\left(v_x \rho \omega_i\right) + \frac{\partial}{\partial y}\left(v_y \rho \omega_i\right) = \varepsilon \rho D_i\left(\frac{\partial^2 \omega_i}{\partial x^2} + \frac{\partial^2 \omega_i}{\partial y^2}\right) + s_i^* \tag{34}$$

for $0 \le x \le a$ and $0 \le y \le b$,

where:

v_x, v_y – velocity vector coordinates $\vec{v}$ on the axes Ox and Oy respectively, m/s, a, b - rectangle dimensions, m,

while the source member present in the equations in the form of (30) is expressed with the following formula:

$$s_i^* = D_i\left[\frac{\partial}{\partial x}\left(\varepsilon \omega_i \frac{\partial \rho}{\partial x}\right) + \varepsilon \frac{\partial}{\partial y}\left(\omega_i \frac{\partial \rho}{\partial y}\right)\right] + M_i \dot{s}_i \tag{35}$$

The positions of porosity in the formula (35) result from the fact that this property, just like permeability k, depends only on the coordinate x.

The origin of the coordinates ($x = 0$, $y = 0$) overlaps with the bottom left corner of the area. In contrast, the axes are pointed in the following directions:

- Ox to the right,
- Oy perpendicular to Ox and following the inlet's airflow direction.

That applies to both simulation variants. The discussed point corresponds to the inlet of the primary airflow, which is also a characteristic shared by both variants. In the second variant, we also consider the airflow through the heading along the upper edge of the area where the coordinate x rises. The possible additional airflow supplied to the headings' intersection (point $x = 0; y = b$) is considered a local mass source's capacity. In both variants the analysis is limited to the flow of a gas mixture of three components ($N = 3$), consisting of nitrogen, ($i = 1$), oxygen ($i = 2$) and methane ($i = 3$). The gas medium's volumetric chemical composition at the inlet ($\xi = y = 0$) corresponds to the atmospheric air composition that is not polluted with methane ($79\% N_2$, remainder O_2). Therefore, the values of mass fractions Ω_i^0 are, $\Omega_1^0 = 0{,}79 \times M_1 / M_p$, $\Omega_2^0 = 1 - \Omega_1^0$ and $\omega_3^0 = 0$ respectively, where $M_p = 0{,}79 \times M_1 + 0{,}21 \times M_2$, kg/mol, denotes the molar mass of unpolluted air.

In addition to the formulated boundary conditions, below we present the connections of the Cartesian variables with the generalized spatial variables ξ and n:

Variant One – the longwall heading is situated along the shorter side of the rectangle, for $x = 0$ which means that $\xi = y$, $\xi_k = b$, $0 \le y \le b$. The formulas (22) and (27) include $n = x$. As for the remaining edges of the area (the other three sides of the rectangle), the boundary conditions (30,31) apply, according to which $n = x$ for the edge ($x = b$) parallel to the axes Oy and $n = y$ for the edges $y = 0$ and $y = b$ parallel to the axis Ox.

Variant Two – in this case, we consider the presence of a longwall heading and a bottom road connected at a right angle in the upper left corner ($x = 0, y = b$) of the goaf area under analysis. An additional airflow can be supplied in the bottom road's rear section, which corresponds to the area's upper horizontal edge. Its mass flow rate, and the partial flows of nitrogen and oxygen, are taken into consideration in the equations (20,26) as local sources of substance. What follows is that initially, a generalized spatial variable ξ runs along the vertical edge, where $\xi = y$ it changes its course in the upper corner to the overlap axis Ox. At this section $\xi = x$. The endpoint, in which the air mixed with methane had its outlet, is defined by the coordinates $\xi_k = a + b$ or $x = a, y = b$. The boundary conditions for the left edge are identical with Variant One. The same holds for the procedure applied at the inlet of air $x = 0, y = 0$, where the boundary condition (22) applies, replacing the variable ξ with y. At the section $y = b, 0 \le x \le a$ in the formulas (22) and (27) surface coordinate normal to the boundary, i.e. n, is replaced with the variable x. For the remaining edges, the conditions (30,31) apply, like in Variant One.

A separate problem is the identification of the substance sources present in the equations (34). The air components' sources, constituting scalar physical fields, are present only in the flows passing through headings and are connected with the filtration in goafs (formulas (27,29)). The remaining sources are connected with the air supply. They have only local character (the cross-sections of inlets into headings, the pipeline's outlet supplying nitrogen into the goaf).

From the perspective of work safety, methane release from the rock mass during the seam's exploitation is highly significant. This process is not homogenous throughout the goaf space, but it is necessary to assume homogeneity for simplification. The fundamental

property used in the calculations is the averaged density of the molar flow of methane supplied to the unit of the horizontal cross-section of the goaf $\dot{r}$, mol/m^2. This property's value, which is treated as constant across the caving horizontal surface, is estimated based on the caving dimensions and the measured values of CH_4 concentration in the air at the mining area outlet. Given the assumption that the model is two-dimensional, the capacity of the sources of methane inside the goaf is:

$$\dot{s}_3 = \frac{\dot{r}}{H} \tag{36}$$

where H – averaged thickness of the goaf (3.5 times the height of the exploited seam), m.

Based on the available capacities of the sources of individual components of the gas mixture, it is possible to calculate the capacity of the whole mass source present in the equations (15,32), using the obvious connection:

$$\dot{s}_m = \sum_{i=1}^{3} M_i \dot{s}_i \tag{37}$$

The formula (37) is also applied when the sources have a local character and possess a dimension mol/s.

The values of the local molar fractions of methane in the gas mixture are determined using the equation (12). Thus, we obtain:

$$\omega_3 = 1 - \omega_1 - \omega_2 \tag{38}$$

The last issue connected with the mathematical model presented here identifies coefficients present in the formula (19) and, consistently, in the equations (21). These equations refer to the individual headings adjacent to the goaf, which means that values E may vary because of their varying geometry affecting the airflow. In the variants under consideration, the number of the listed headings is: one in Variant One, which means that only a single coefficient needs to be known E, and two in Variant Two, were both listed coefficients, i.e. E_1 and E_2, need to be present. The coefficient E_1 corresponds to the section of the heading parallel to the axis Oy, whereas the coefficient E_2 corresponds to the section parallel to the axis Ox. The listed coefficients' values are available in the existing literature and need to be treated as the model's so-called *selectable parameters*. They can be determined with some degree of approximation, using values of pressure measured locally along the headings' length. By variating the values E, it is possible to match optimally the theoretical curve obtained as a numerical solution to the equation (21) to collect measuring points by using the least-squares method. The fragment of the numerical procedure corresponding to this stage of the calculations will be the subject of the next subchapter of the article.

4.4 The description of the applied numerical method

The applied calculation algorithm consists of two parts. The first part concerns the determination of the distributions of pressure p and mass fractions of the components of the gas mixture ω_i in the area under consideration; this area encompasses the goaf with the adjacent headings, through which the air supplied to the mining area flows.

The other part of the procedure concerns estimating the selectable parameters E, whose averaged values determine air pressure distribution along the heading, given the inlet's mass flow density (20). As has already been mentioned, values of pressure measured along the heading's length are used for this purpose. Below we include an abridged description of the numerical procedures applied.

5 RESULTS AND DISCUSSION

5.1 The determination of discrete pressure fields and the concentrations of the components of the gas mixture

The Control Volume Method (CVM), employed to find a numerical solution to the problem with boundary conditions described in the previous subchapter, was described in detail in Chapter 5 of V. S. Patankar's monograph [21]. At this point, we provide only a summary of his argument, while simultaneously drawing attention to the differences between the form of particular equations in V. S. Patankar's study and the present article. In the preliminary phase, V. S. Patankar [21] uses generalized properties, i.e. introduces the notions such as the generalized scalar field ϕ responsible for transport, the Generalized Extensive Property (GEP), e.g. energy represented as heat or amount of substance. In the most general case, a process can have a non-stationary character, so the equations contain the so-called temporal derivative '$\partial / \partial t$', where t – time, s. The author limits the presentation to equations within the Cartesian coordinate system; to make the equations more concise, he uses the summation convention, replacing the coordinates *x, y, z* with a generalized coordinate x_j ($j = 1,2$ in the case of 2-D). Also, he applies the notion of generalized dynamic diffusivity Γ, treated as a variable. The medium's linear velocity is marked as $\vec{u}$, while its coordinates on the axes are designated as u_j. In the present article $\phi \equiv p, c_i$, $\Gamma_i = \rho D_i$, $i = 1,2,3$ (while $D_i \cong const$), and the equations (34) and (32) correspond to the ones proposed by Patankar [21]. However, he leaves the presence of the external sources of substance out of consideration. The presented differential equations are strongly non-linear, and an analytical (exact) solution is not available. For this reason, it is necessary to find an approximate discrete solution by covering the area under analysis with the so-called *numerical grid*. The field values are calculated in selected points, which constitute *grid points*. The nodes of the numerical grid can be equidistant, or the distances between them, referred to as *integration steps*, can vary. It is worth noting that those values simulate the differentials of spatial variables *dx* and *dy*. If the invariability of the steps mentioned above applies to each of the coordinate system's discussed axes, the grid is called a *regular grid*. Numerical grids corresponding to the equations written in the Cartesian system are known colloquially as *Cartesian grids*.

Each node in the grid is situated within a 'mini area' called *Local Control Volume* (LCV), which is also known under the term *elementary rectangular prism* in Cartesian grids. The individual LCVs are in contact with one another, exchanging balanced extensive property via shared interfaces. The transfer, which discussed here has a convectional-diffusive character, occurs in one dimension (1-D) through channels running along axes between neighbouring nodes. The length of the channels is equal to the length of each integration step. In Cartesian grids, each channel's cross-section area is constant along its length and equal to the neighbouring control volumes' contact surface area. The surface elements separating adjacent control volumes cut across integrations steps at half their length.

The applied approximation rests on two fundamental assumptions:

- The resultant physical field ϕ is homogenous (has a constant value) within a single LCV, but changes abruptly at the neighbouring volumetric element's contact surface.
- Linear variability ϕ is assumed to exist along a single channel linking two neighbouring nodes of the grid, which makes it possible to calculate the values of parameters depending on this function, e.g. ρ or Γ, or at any point of the integration step, by linear interpolation.

Inside the volumetric element LCV, there is a *central point* designated as P, while the *neighbouring points* are designated as N, W, S, E, respectively. Consequently, the points where integration steps cut across contact surfaces are designated with small letters (n, w, s, e). In these points, the fluxes density *coordinates* of the balanced GEP are defined, whereby the appropriate differential quotients replace the derivatives of the first order. In V. S. Patankar's study [21], the two cases are referred to as 1-D and 2-D. After producing a complete notation of the balance for the second case, including the balances of all inflows and outflows and the internal production and accumulation of the transferred GEP, we obtain a single discrete equation. It is immediately evident that the number of such equations for the entire area corresponds precisely to the assumed number of nodes, i.e. also the amount of LCV. Discrete equations are not formulated only for nodes situated at an edge, where values for a field are given directly (the so-called *Dirichlet boundary condition*). After the appropriate transformations and simplifications, we obtain a system of discrete equations with the following general form:

$$a_W\phi_W + a_E\phi_E + a_S\phi_S + a_N\phi_N - a_P\phi_P + b = 0 \tag{39}$$

where:

a_{O} - coefficients concerning the neighbouring nodes ($\mathrm{O} \equiv W, E, S, N$),

b - free term.

The member b and the coefficient a_P for the 2-D case are defined in W. D. Patankar's study [25] with appropriate formulas. In both formulas mentioned above, we find the element a_P^0 connected with the accumulation of GEP (whose value is zero in stationary contexts), as well as members resulting from the linearization of the function, which defines the possible dependence of the efficiency of the internal source of GEP on ϕ. The linearization described above is recommended because, in no small extent, it guarantees the convergence of the iterative process. The properties Δx , Δy refer to the integration steps along the axes x and y.

The number of discrete equations in the system is closely connected with the grid's density, and solving the system leads to determining the field's values ϕ for particular nodes. However, the presented method of calculation has its limitations because of the so-called *convergence* and *numerical stability*. Evidence is provided that the convergence and physical solution accuracy basic condition is to satisfy the inequality presented below for every LCV belonging to the grid, at every stage of the calculations:

$$a_{\mathrm{O}} \geq 0 \quad \text{for} \quad \mathrm{O} \equiv W, E, S, N \tag{40}$$

It is easily proven that if the transfer of GEP is limited to diffusion throughout the entire area, the condition (39) is always fulfilled, regardless of the numerical grid's density (V. S. Patankar) [21]. The possible non-fulfilment of the condition results only from the presence of convection in the area around point P. In V. S. Patankar's study [21], we find a presentation of an approximation of GEP flows (for the 1-D case, ϕ a stationary field), which after the appropriate transformations produces a discrete equation. An analysis of the formulas included in the monograph reveals that the coefficients a_W and a_E can assume negative values contrary to the condition (40); this causes results to oscillate at an early stage of the calculations, and later leads to the divergence of the numerical procedure. Satisfying this condition is possible only for grids with a tiny integration step, particularly when the transfer of GEP is strongly dominated by convection, i.e. is characterized by high local values of linear velocity.

A similar analysis was presented for a two-dimensional 2-D field ϕ and a non-stationary field [21], where the velocity vector in the Cartesian system was designated with the elements u and v. The equation expressing the elementary balance of GEP contains a cumulative member, the balance of GEP flows calculated based on their densities expressed by appropriate formulas, and the source member. The equation corresponds to LVC having a form of an irregular Cartesian grid presented in a figure in the quoted monograph [21]. The GEP flows densities are defined on the LVC surface. That imposes a necessity of defining the values of u and v in those places. Homogenous distribution of the properties mentioned above is assumed on the surfaces across which GEP is transferred. The right-hand side of V. S. Patankar's equation [21] presents an internet source of GEP in a linearized form, which – as has already been said – is recommended if S is a function of ϕ. It is easy to notice that also in this case the coefficients a_{O} can have negative values if the densities of convection flows on the boundary surfaces of LVC are approximated in a way described in this source [21]. It mainly refers to a situation in which the transfer of GEP occurs through convection, while the direction of the velocity vector is subject to change. To guarantee that the condition (40 and 36) is met, the convection-related terms in generalized equations are approximated using procedures based on the UPWIND scheme. The essence of the procedure is described in detail V. S. Patankar's study [21]. It consists in using a different density vector coordinates approximation of the GEP convection flow. In case of 2-D they are determined along Ox LCV lateral surfaces direction as $(u\phi)_w = u_w\phi_W \cap (u\phi)_e = u_e\phi_P$, for $u_w > 0 \cap u_e > 0$ and as $(u\phi)_w = u_w\phi_P \cap (u\phi)_e = u_e\phi_E$ accordingly for $u_w < 0 \cap u_e < 0$. In the case of direction Oy, an analogous approximation procedure is applied, taking into account the velocity v element. Therefore, the value ϕ_o calculated by linear interpolation between the values ϕ_P and ϕ_{O} is substituted with only one of the mentioned properties. The choice of the value for this substitution depends only on whether the coordinates on the corresponding lateral surfaces of the LCV are positive or negative. The listed coordinates are given general designations as u_o for $o \equiv w,e$ and as v_o for $o = s,n$.

In V. S. Patankar's monograph [21], some improvements to the UPWIND procedure were proposed and named HYBRID and POWER LAW. Here, the approximation is based on the so-called *exact solution*. It is an analytical solution to the equation of convection-diffusion transfer for the source-free case 1-D. It concerns the above-discussed channels through which GEP is exchanged between neighbouring LCV. This solution is applied in the case with the Dirichlet boundary conditions on both sides of the channel. It rests on the assumptions that

the transfer is one-dimensional and no internal sources of GEP exist, which – as we already know – are crucial for the CVM method. In the quoted monograph [21], the solution is presented as a formula containing an important dimensionless parameter known as the Péclet number. The number, usually designated in the literature on chemical engineering as Pe_{n} and by V. S. Patankar [21] as P, is an important criterion defining the degree to which the combined (convection-diffusion) transfer is dominated by convection. This criterion is defined with the assumption that both convection and diffusion occur in the same direction. Because the channel length, designated in V. S. Patankar's study [21] as *L,* m, is in the 2-D case equal to the corresponding integration steps, Δx or Δy, in the present article it is possible to give it the following generalized definition:

$$P_{\xi} = \frac{v_{\xi}\Delta\xi}{\varepsilon D} \quad \text{for} \quad \xi \equiv x, y \tag{41}$$

In the procedures proposed by V. S. Patankar [21], the terms of the equation related to diffusion are neglected for $P > 10$, and only the terms related to convection are considered. The POWER LAW scheme applied in the simulation presented here consists in replacing the terms containing the function '$\exp(P)$', obtained from the exact solution, with the function '$(1-0{,}1|P|^5)$', which significantly reduces the workload during computer-assisted calculations. A detailed notation of the formulas defining the discrete equation's coefficients in the 2-D case for the POWER LAW scheme can be found in the set of relevant formulas presented by V. S. Patankar [21].

Therefore, the UPWIND procedure's application makes it possible to disregard the numerical grid's density and is particularly important in the two- (or possibly three-) dimensional contexts. The time needed for the calculations and the RAM workload are strongly dependent on the integration steps' size in both of them. The inevitable cost is lowering the so-called *degree of approximation*, which reduces the calculations' accuracy and causes undesirable *false diffusion* in the numerical grid [21]. However, in practice, the obtained accuracy is satisfactory for the numerical simulation of the convection-diffusion transfer relevant from the technological perspective. Transferred GEP global balance results confirm that for the entire area under analysis based on the field ϕ's values and possible experimental research.

Above, we have presented the order of numerical actions for the implemented calculation procedure. The sequence of operations to be carried out is as follows:

1. Providing input data (the appropriate numerical values); the number of numerical nodes along the particular axes of the coordinate system, the geometrical dimensions of the goaf area and headings, the data concerning the permeability of the goaf, the capacity of the external sources of methane homogenous throughout the goaf area, the local capacity of the source of nitrogen at the outlet of the supply pipeline, the linear velocity of airflow and the volumetric chemical composition of air at the inlet into the heading, the physical properties of the individual gas components (molar mass, dynamic viscosity, kinematic diffusion coefficient).
2. Generating a numerative grid numerically.
3. Defining the values of permeability inside the goaf on the surfaces separating individual control volumes.
4. Defining preliminary approximations of the physical fields to be determined to provide a basis for iterative calculations.

5. The subsequent stages of the iterative process:
    - Defining the gas mixture's physical properties, such as density (17) and dynamic viscosity (Wilky's algorithm) both at the grid's nodes and on the surfaces separating individual control volumes.
    - Determining the discrete pressure field by solving numerical equations (32) and (21).
    - Calculating the coordinates of the vector of the linear velocity of the gas medium using Darcy's formulas (33) and the pressure field defined in point "b".
    - Calculating the discrete fields of the mass fractions of nitrogen and oxygen inside the goaf and in the headings using the formulas (34) and (26).
    - Calculating the discrete field of the mass fraction of methane inside the goaf and in the headings using the formula (38).
    - Interpreting the results obtained in points 'b-e' as another approximation and returning to point 'a'.

The pressure field's numerical values and the mass fractions of nitrogen and oxygen are calculated by solving a certain algorithm TDMA (Tridiagonal Matrix Algorithm) [21]. The iterative process is interrupted when the fields' obtained values to be determined change to a negligibly small degree (below the acceptable measurement error).

5.2 Determination of the values of selectable parameters concerning the airflow along with the heading

The algorithm presented in the previous subchapter makes it possible to determine gas mixture components' pressure and mass fraction fields for the given values of E (19), both inside the goaf and along the headings. This value, which to some extent provides a measure of air flowing along a heading permeability, determines (given the inlet mass flow rate) the overpressure Π value at the inlet. As a consequence, we get the shape and the inclination of the curve $\Pi(\xi)$ towards the outlet. As has already been mentioned, the E values should be determined based on measurement data forming an experimental picture of the distribution mentioned above in a discrete form, i.e. elements of the sequences Π_k^0 and ξ_k^0. The k index is attributed to a given measurement point, ($k = 1,2,...,K$), while K denotes the number of these points along the coordinate ξ. The values ξ_k^0 corresponding to the heading cross-sections for which the pressure has been measured usually do not overlap with the numerical grid's nodes. To achieve an optimal approximation of the distribution $\Pi(\xi)$ obtained numerically to the corresponding experimental data, the following function is considered:

$$\Phi = \sum_{k=1}^{K} \left[\Pi(E_1, E_2, ..., \xi_k^0) - \Pi_k^0 \right]^2 \tag{42}$$

where the values E_1, E_2 are parameters present in the equations (19), written in a sequence for headings numbered 1, 2, etc. In Variant One with a single heading, $\Pi(E)$ is present only, whereas, in Variant Two, two headings (a longwall heading and a bottom entry) perpendicular to each other are considered and it is necessary to take into account $\Pi(E_1, E_2)$. In the second case, the indicator '1' denotes a heading following the axis Oy, whereas the indicator '2' points to the heading parallel to the axis Ox.

The function $\Pi(\xi)$, whose values are calculated only in the grid's nodes, is also discrete, which means that numerical values for intermediate points are not available.

Nevertheless, the data listed above can be determined with sufficient accuracy by applying linear interpolation and introducing linear functions to define overpressure Π for the sections between the nodes. Thus, we obtain a complex function, represented graphically by a polyline. The mathematical notation of this function is as follows:

$$\Pi(E_1, E_2, ..., \xi_k^0) = \Pi_i - \frac{\Pi_i - \Pi_{i+1}}{\Delta\xi}\left(\xi_k^0 - \xi_j\right) \tag{43}$$

for $\xi_j \le \xi_k^0 < \xi_{j+1}, \xi_{j+1} = \xi_j + \Delta\xi$,

where:

$\Delta\xi$ - distance between the nodes, m,

j - a discrete variable attributed to a given node of the grid on the coordinate ξ, $j = 1,2,...,J$,

J - the number of listed nodes along the coordinate.

Evidence is given that the expression (42) defined as a function of only parameters E for the given set of experimental data has only one minimum. This is because dependence $\Pi(\xi)$ is always monotonic. After all, the overpressure values decrease in the flow direction. This means that it is possible to match the distribution $\Pi(\xi)$ achieved through calculations to the appropriate experimental values by manipulating values E correctly. Therefore, the procedure described above is an example of applying the well-known least squares method, in which the values of the function approximating experimental data are defined only numerically. However, the procedure requires repeated determination of the components' discrete fields of pressure and molar fractions. It is done based on the procedure described in subchapter 5.1, and it means that the calculations are more time-consuming.

The numerical methodology applied for Variant One to determine the minimum mentioned above is also iterative. It consists of calculating three consecutive values of the function Φ based on the formulas (42,43) for three consecutive values of E, which differ by a constant, initially assumed step value ΔE. Before beginning the preliminary calculations values E and ΔE are determined. The first stage of the procedure involves investigating whether finding the desired minimum requires increasing or decreasing the value E. If for the first 'trio' of E argument *values* introduced in ascending order, we obtain a corresponding sequence of values Φ in descending order, the iterative process is continued by increasing all three arguments' values until the second element in the sequence Φ reaches a value smaller than the two others. This can be expressed with the following system of inequalities:

$$\Phi_2 < \Phi_1 \cap \Phi_2 < \Phi_3 \tag{44}$$

At this point, the iterative process is stopped, while the value $E_{\min}$ corresponding to ' $\min\Phi$ ' is approximated by calculating the vertex's position of the parabola containing all the three points with the coordinates ' $E_l, \Phi(E_l)$ ', $l = 1,2,3$. The equation of this parabola is determined using the Lagrange polynomial.

On the other hand, the inverse case, in which an increase of the values Φ along with the rising E is implied, means that the initially assumed value of the argument is an overestimation. This in turns requires gradual decreasing by the value ΔE until the expected result is achieved: a system of inequalities (43). In this case, a sequence of three elements E_l

for $l = 1,2,3$ is a decreasing one during the search of ' $\min \Phi$ '. After achieving the result (40), the value $E_{\min}$ is calculated exactly as before.

As for Variant Two, for which $\Phi = \Phi(E_1, E_2)$, where the selectable parameters E_1 and E_2, which are arguments of the function Φ, refer to two headings perpendicular to each other, a necessity exists to search for a minimum of the function with two independent variables. Unfortunately, this minimum takes a much longer time to calculate. Like for Variant One, to determine the value E_2, $E_{1\min}$ is defined. Furthermore, $E_{2\min}$ is calculated, with the assumption that the previously calculated value $E_1 = E_{1\min}$ does not vary. Determining the constant values $E_{1\min}$ and $E_{2\min}$ the way described above is repeated until the satisfactory accuracy of calculating $\min \Phi$ is achieved. The final obtained values of the constants E with their corresponding discrete fields Π, π, Ω_i and ω_i for $i = 1,2,3$, are the final result of the calculations.

5.3 Results of the proposed model used on the example of two discussed variation of longwall mining.

To illustrate the mathematical model, sample calculations were carried out for the two discussed variants of longwall mining in a coal seam.

For Variant One (a longwall with a U-shaped ventilation system) the following geometrical dimensions of the longwall were assumed: the longwall length 200 m, the life of the longwall for which the calculations were carried out was 420 m. The thickness of the extracted seam was 2.0 m, and the flow rate of the supplied fresh air was 1200 m^3/min, the thrust loss being equal to 130 Pa. It was assumed for the calculations that the separation resistance of the rocks in the roof was 2.0 MPa, which is typical of a weak roof, with cracks, and easily caved in. Such roofs consist of rocks such as mudstone. The amount of methane released into the goaf under consideration was 10 m^3/min CH_4.

Results obtained from calculations made by the programmes created for the purpose are shown in Figures 7a,7b,7c and 7d where:

- Figure 7a - isoline map of methane concentration distribution in the goaf,
- Figure 7b – isoline map of oxygen concentration distribution of in the goaf,
- Figure 7c - isoline map of air velocity distribution in the goaf,
- Figure 7d - the air velocity the vector distribution in the goaf.

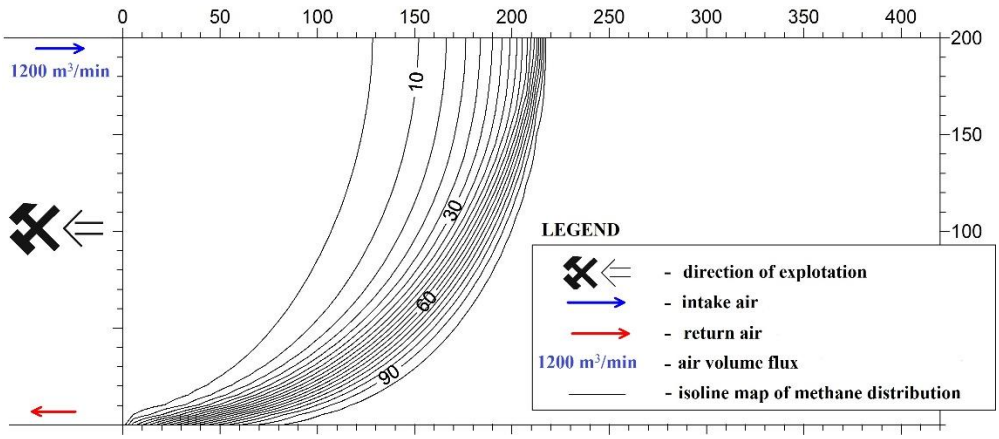

methane,%

Fig 7a. Isoline map of methane concentration distribution in the goaf with a U-shaped ventilation system

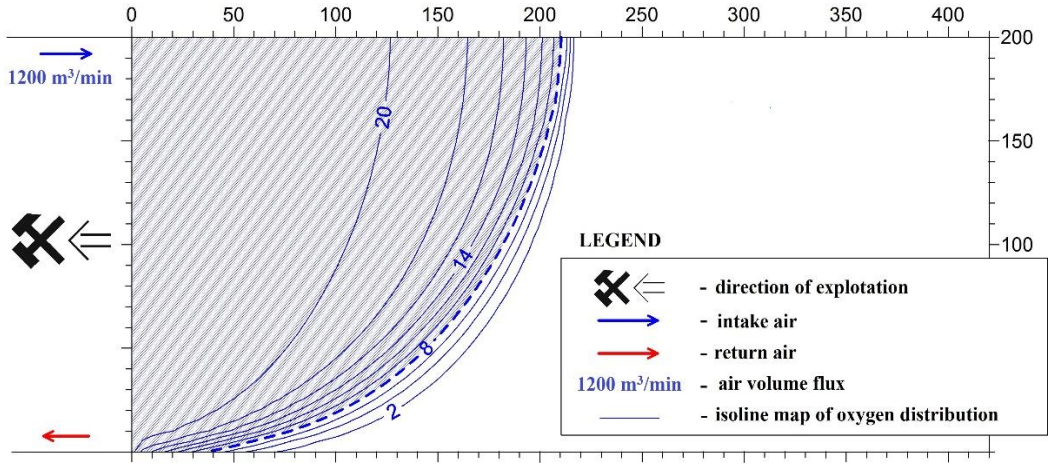

oxygen, %

Fig 7b. Isoline map of oxygen concentration distribution in the goaf with a U-shaped ventilation system

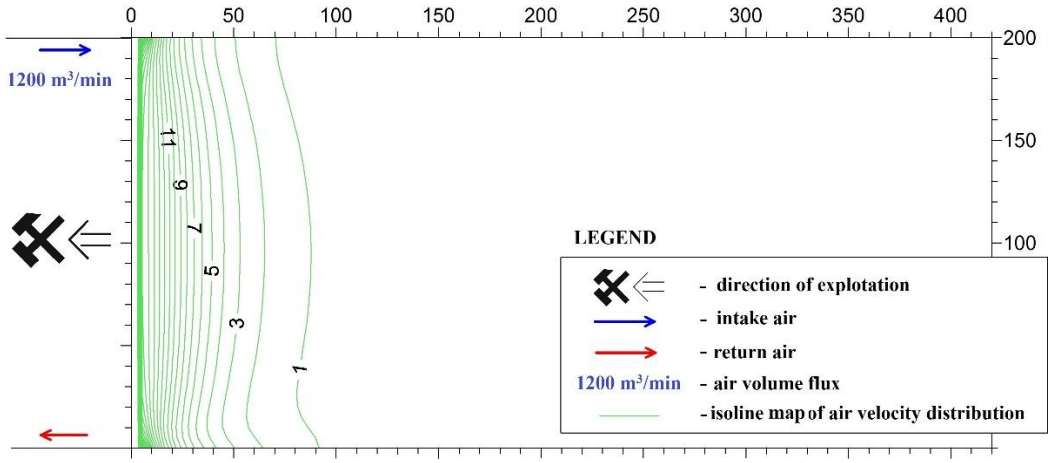

velocity, mm/s

Fig 7c. Isoline map of air velocity distribution in the goaf with a U-shaped ventilation system

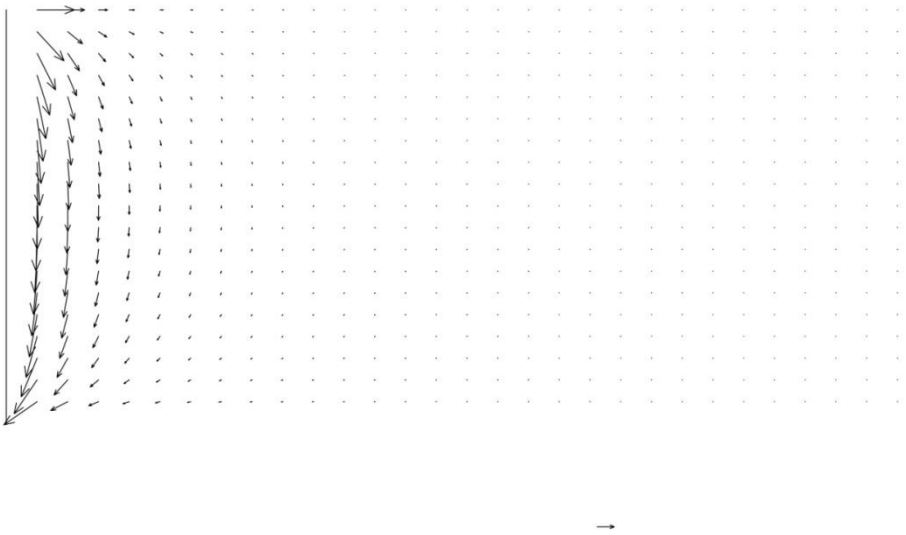

velocity – vectors (length of the reference vector 10 mm/s)

Fig 7d. The vector distribution of air velocity in the goaf with a U-shaped ventilation system

For Variant Two (a longwall with a Y-shaped ventilation system) the following geometrical dimensions of the longwall were assumed: the longwall length 200 m, the life of the longwall for which the calculations were carried out was 600 m. The thickness of the extracted seam was 2.0 m, and the flow rate of the supplied fresh air was 1200 m^3/min, the thrust loss was equal to 130 Pa. The air outlet from the longwall was also ventilated with a flow rate of 600 m^3/min of fresh air. The thrust loss in the bottom entry was 30 Pa. It was assumed for the calculations that the separation resistance of the rocks in the roof was 2.0 MPa, which is typical of a weak roof, with cracks, and easily caved in. Such roofs consist of rocks such as mudstone. The amount of methane released into the goaf under consideration was 10 m^3/min CH_4. Results obtained from calculations made by the programmes created for the purpose are shown in Figures 8a,8b,8c and 8d where:

- Figure 8a - isoline map of methane concentration distribution in the goaf,
- Figure 8b – isoline map of oxygen concentration distribution of in the goaf,
- Figure 8c - isoline map of air velocity distribution in the goaf,
- Figure 8d - the air velocity the vector distribution in the goaf.

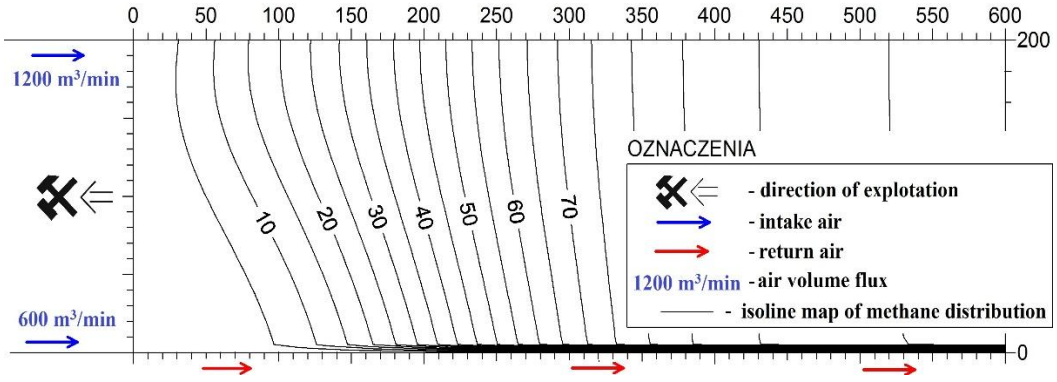

methane, %

Fig 8a. Isoline map of methane concentration distribution in the goaf with a Y-shaped ventilation system

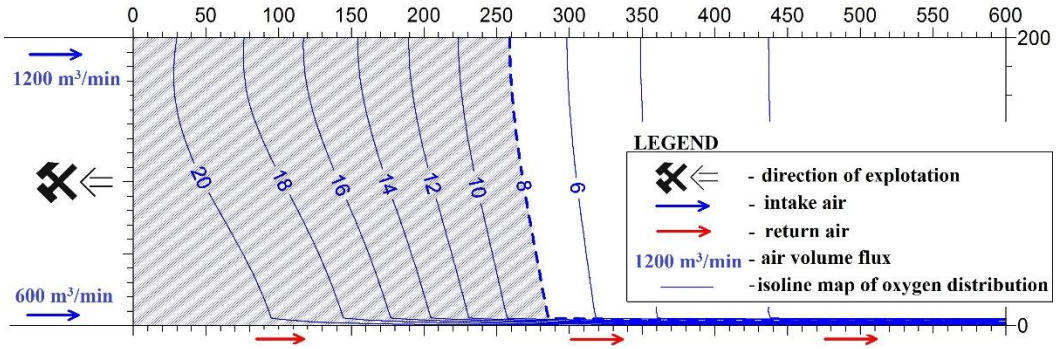

oxygen, %

Fig 8b. Isoline map of oxygen concentration distribution in the goaf with a Y-shaped ventilation system

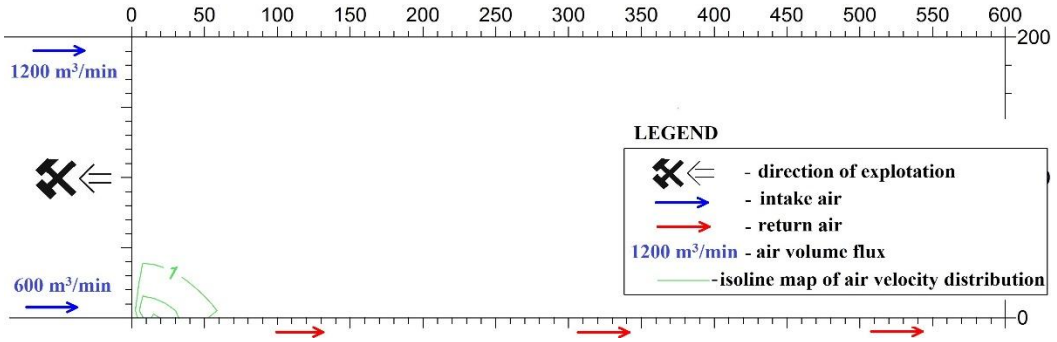

velocity, mm/s

Fig 8c. Isoline map of air velocity distribution in the goaf with a Y-shaped ventilation system

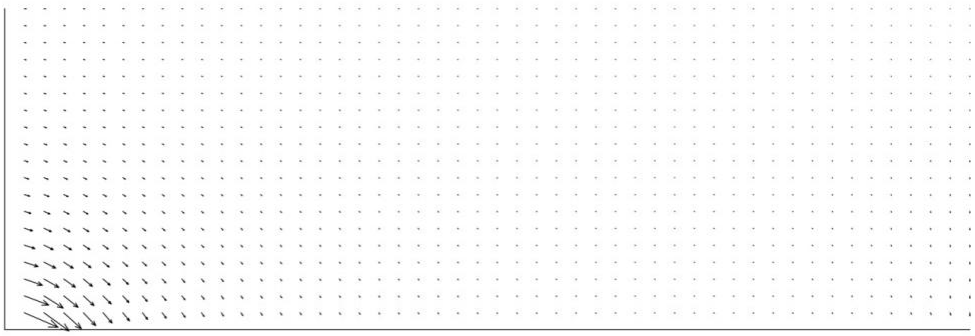

velocity – vectors (length of the reference vector 10 mm/s)

Fig 8d. The vector distribution of air velocity in the goaf with a Y-shaped ventilation system

6 CONCLUSION

The article presents a simulation of the movement of substance within a porose structure left by the complete extraction of a coal seam through longwall mining in an underground mine. The resultant goaf, which remains after a coal seam has been exploited, can be interpreted as a horizontally oriented, rectangular slab with the horizontal dimensions x and y and the vertical dimension 3.5m, where m denotes the thickness of the extracted seam.

In this area, the filtration of air supplied by the mine's ventilation system occurs, reaching the place through headings adjacent to the horizontal edges of the rectangular block. Inside the goaf, in a porose space, the inevitable complex processes of carbon oxidation occur, and methane is released from the layers permeated with methane.

The calculations also consider the local nitrogen emission with a given volume flow rate, supplied via a pipeline to the inside of the caving along the longer edge of the area. The simulation yields the following two-dimensional discrete (2-D) physical fields present in the space of the caving:

- pressure increase field
- field of the apparent velocity of the mixture of the components
- field of the molar concentration of nitrogen N_2
- methane concentration field CH_4
- oxygen concentration field O_2

The obtained calculation algorithm is based on a *Control Volume Method* procedure, which in Poland has also been referred to as the *Elementary Balance Method.*

They created computer programmes that enable the determination of the fields mentioned above in two variants with different boundary conditions. The calculated results make it possible to predict the gas mixture's explosiveness in the goaf containing methane and the distribution of oxygen content, causing the oxidation of the remnants of coal in the goaf.

Author Contributions: Author Contributions: J.S. (65%): developed a methodology for the presentation of research results, contributed analysis tools, analyzed data, and wrote the paper. N.S. (35%): developed a concept for the presentation of research results. All authors have read and agreed to the published version of the manuscript.

Funding:

Informed Consent Statement: Informed consent was obtained from all subjects involved in the study

Data Availability Statement: Upon authors' request

Conflicts of Interest: The authors declare no conflict of interest.

7 REFERENCES

[1] Szlązak, J. Przepływ powietrza przez strefę zawału w świetle badań teoretycznych i eksperymentalnych. Uczelniane Wydawnictwa Naukowo-Dydaktyczne AGH: Kraków, Poland, 2000. (In Polish)

[2] Dieu, N.H. Metoda prognozowania rozkładu koncentracji metanu w zrobach ścian zawałowych. A doctoral dissertation. Politechnika Śląska: Gliwice, Poland, 1994. Unpublished. (In Polish)

[3] Kelsey, A.; Lea, C. J.; Lowndes, I. S.; Whittles, D.; Ren, T. X. CFD modelling of methane movement in mines. 30th International Conference of Safety in Mines Research Institutes, South African Institute of Mining and Metallurgy 2003, 475-486.

[4] Wala, M.A.; Vytla, S.; Taylor, C.D.; Huang P.G. Mine Face ventilation: a comparison of CFD results against benchmark experiments for the CFD code validation. Mining Engineering 2007, 59/10.

[5] Szlązak J. Wpływ uszczelnienia chodników przyścianowych na przepływ powietrza przez zroby. A doctoral dissertation. AGH: Kraków, Poland, 1980. Unpublished. (In Polish)

[6] Szlązak J. The determination of a co-efficient of longwall gob permeability. Arch. Min. Sci. 2001, 46, 451-468.

[7] Tauziède, C.; Mouilleau, Y.: Bouet, R. Modelling of gas flows in the goaf of retreating faces. 25th Conférence Internationale des Instituts de Recherches sur la Sécurité dans les Mines: Pretoria, South Africa, 1993.

[8] Ferziger, J. H.; Perić, M. Computational Methods for Fluid Dynamics. Springer: Berlin, Heidelberg, New York, 2002. doi 10.1007/978-3-642-56026-2

[9] Ren, T.X.; Edwards, J.S. Three-dimensional computational fluid dynamics modelling of methane flow through permeable strata around a longwall face. Min. Tech. 2000, 109, 41-48.

[10] FLAC3D, 2014. FLAC –Available online: https://www.itascainternational.com/software/flac3d

[11] Esterhuizen, G.; Karacan, C.Ö. Development of numerical models to investigate permeability changes and gas emission around longwall mining panels. Proc. Alaska Rocks, 40th US Symposium on Rock Mechanics: Anchorage, Alaska, 25-26 June 2005

[12] Karacan, C.Ö.; Diamond, W.P.; Esterhuizen, G.S.; Schatzel, S.J. Numerical Analysis of the Impact of Longwall Panel Width on Methane Emissions and Performance of Gob Gas Ventholes. Proc. Int. Coalbed Methane Symp., 18-19 May, Paper 0505. Tuscaloosa, Alaska 2005.

[13] Esterhuizen, G.; Karacan, C.Ö. A methodology for determining gob permeability distributions and its application to reservoir modeling of coal mine longwalls. SME annual meeting: Denver, USA, 2007.

[14] Karacan C.Ö. A new method to calculate permeability of gob for air leakage calculations and for improvements in methane control. Proceedings of the 13th

U.S./North American Mine Ventilation Symposium., June 13-16: Sudbury, Ontario, Canada, 2010, 273-282.

[15] Karacan C.Ö. Prediction of Porosity and Permeability of Caved Zone in Longwall Gobs. Transport in Porous Media 2010, 82, 413-439.

[16] Znański, J. Podziemna eksploatacja złóż - część I. Wydawnictwa AGH: Kraków, Poland, 1961. (In Polish)

[17] Mileticz, A.F. Utieczki wozducha i ich razcziet pri prowietriwanii szacht. Moskva, Russia, 1963.

[18] Szlązak, J. Wpływ uszczelnienia chodników przyścianowych na przepływ powietrza przez zroby. A doctoral dissertation, AGH; Kraków, Poland, 1980. Unpublished. (In Polish)

[19] Szlązak ,N; Szlązak, J. Filtracja powietrza przez zroby ścian zawałowych w kopalniach węgla kamiennego. Uczelniane Wydawnictwa Naukowo-Dydaktyczne AGH: Kraków, Poland, 2005. (In Polish)

[20] Pohorecki, R, Wroński, S. Kinetyka i termodynamika procesów inżynierii chemicznej. Wydawnictwa Naukowo-Techniczne: Warszawa, Poland, 1979. (In Polish)

[21] Patankar, S.V. Numerical Heat Transfer and Fluid Flow. Hemisphere, Mc Graw-Hill: Washington D.C. USA, 1980.

[22] Kłeczek, Z. Geomechanika górnicza. Śląskie Wydawnictwo Techniczne: Katowice, Poland, 1994. (In Polish)

[23] Ropski, S. Stan pełnego i wysokiego zawału oraz stref osiadania stropu za ścianą na podstawie pomiarów w kopalni „Wesoła" w pokładzie 329. A doctoral dissertation, AGH: Kraków, Poland 1964. Unpublished (In Polish)

[24] Puczkow, Ł.A. Aerodynamika podziemnych wyrabotanych prostranstw. Gornyje Nauki: Moscva, Russia, 1993.

[25] Malczewski, J.; Piekarski, M. Modele procesów transportu masy, pędu i energii. Wydawnictwa Naukowe PWN: Warszawa, Poland, 1992. (In Polish)

[26] Szlązak, J.; Szlązak, N. Numerical determination of methane concentration in goaf space. Arch. Min. Sci. 2004, 49, 587-599.

[27] Szlązak, J. The determination of a co-efficient of longwall gob permeability. Arch. Min. Sci. 2001, 46, 451-468.

Numeryczne wyznaczanie pól prędkości i koncentracji gazu

w przestrzeni zrobów podziemnej kopalni węgla kamiennego

STRESZCZENIE

W pracy opracowano numeryczny model przepływu i składu gazu w zrobach powstałych po wydobyciu węgla metodą ścianową. Zroby traktowane są jako pozioma, prostokątna, porowata płyta o grubości równej 3,5-krotności grubości wyeksploatowanego pokładu. Powietrze z systemu wentylacyjnego kopalni napływa do tego obszaru porowatego przez sąsiednie wyrobiska, podczas gdy metan uwalniany jest z warstw metanowych, a utlenianie węgla zachodzi w gruzie. Model obejmuje również lokalne wtryskiwanie azotu o określonym przepływie objętościowym rurociągiem wzdłuż długiej krawędzi zrobów. Wykorzystując metodę objętości kontrolnej (Control Volume Method), autorzy obliczają dwuwymiarowe pola dyskretne w zrobach: nadciśnienie, pozorną prędkość mieszanki gazowej oraz stężenia molowe azotu, metanu i tlenu. Powstałe programy komputerowe określają te pola dla dwóch układów wentylacyjnych, odpowiadających typowym układom stosowanym w górnictwie ścianowym, z których każdy ma odmienne warunki brzegowe. To podejście umożliwia ilościową ocenę migracji i wzorców dystrybucji gazu w strefie zawału, wspierając projektowanie wentylacji i ocenę zagrożeń metanem i tlenem.

SŁOWA KLUCZOWE: pole prędkości, mieszanina gazów, model numeryczny, przestrzeń zrobowa